Available online at www.sciencedirect.com
SCIENCE DIRECT®
Journal of Sound and Vibration 294 (2006) 278–297
JOURNAL OF SOUND AND VIBRATION
www.elsevier.com/locate/jsvi

Semi-analytic solution in the time domain for non-uniform multi-span Bernoulli–Euler beams traversed by moving loads

A.E. Martínez-Castro, P. Museros*, A. Castillo-Linares

Departamento de Mecánica de Estructuras, E.T.S. Ingenieros de Caminos C. y. P., Campus de Fuentenueva, Universidad de Granada, 18071-Granada, Spain

Received 5 February 2004; received in revised form 15 August 2005; accepted 14 November 2005
Available online 18 January 2006

Abstract

This paper presents a semi-analytic solution of the moving load problem which is of great interest for the analysis of multi-span uniform and non-uniform beams subjected to moving forces, such as high-speed trains. The solution is based on the response of the structure to a unit load circulating at a constant speed of the train. Viscous modal damping is considered. Using Bernoulli–Euler beam elements with variable cross-sectional properties, the structure is discretized and the mode shapes are computed using standard procedure. The moving load is represented by a unitary Dirac Delta function, and the modal loads are obtained in terms of cubic Hermitian polynomials. This leads in a straightforward manner to the closed-form solution for the unit load in the time domain. The solution is expressed in terms of 10 coefficients per element and per mode, the values of which are independent of the speed of the moving load. Finally, the response to a series of loads is built simply by adding the contribution of each. The overall procedure is fast and accurate, depending only on the spatial discretization and the time step selected for evaluating the solution without the need of any integration step. Numerical tests have been included in order to show the efficiency of this technique.

1. Introduction

The dynamic behaviour of beams under moving loads is of great importance in several fields of engineering, for instance, the design of road and railway bridges and the analysis of machining processes. Many engineers and scientists have contributed to the solution of the problem with their innovations, and still the dynamics of beams when subjected to moving loads is a subject that draws considerable attention of researchers.

The present paper is aimed at the analysis of the response of Bernoulli–Euler beams subjected to flexural vibrations under the presence of concentrated moving forces. This topic, which is central to the analysis of railway bridges, has become a particular focus area of research because of the appearance of ballast destabilization problems in some European high-speed rail lines. The committee D-214 of the European Rail Research Institute endeavoured to analyse these problems, and some of the conclusions of its work were

*Corresponding author. Tel.: +34 958 24 07 68; fax: +34 958 24 99 59.
E-mail addresses: amcastro@ugr.es (A.E. Martínez-Castro), pmuseros@ugr.es (P. Museros), acastillo@acl-estructuras.com (A. Castillo-Linares).

0022-460X/$ - see front matter © 2005 Elsevier Ltd. All rights reserved.
doi:10.1016/j.jsv.2005.11.009

Nomenclature

$w(x,t)$	deflection of the beam
$p(x,t)$	load function
$p_k(x)$	$k-$ load of a train, modelled as a set of concentrated forces
p_0	single concentrated load acting on the beam
v	speed of the train
$\delta(x)$	Dirac delta function
l^e	length of element e
E	modulus of elasticity of the beam
$I(x)$	second moment of area of the cross-section of the beam
I_i^e, I_j^e	second moment of area of the cross-section at the beginning and end nodes of element e
A_i^e, A_j^e	area of the cross-section at the beginning and end nodes of element e
d_i^e, d_j^e	equivalent height at the beginning and end nodes of element e
m_i^e, m_j^e	mass per unit length at the beginning and end nodes of element e
γ	permanent added mass
$m(x)$	mass per unit length
$\mathbf{y}(t)$	time-dependent vector of nodal displacements/rotations
$\mathbf{M}^e$	element mass matrix
$\mathbf{M}$	global mass matrix
$\mathbf{M}_D$	diagonal global mass matrix
$\mathbf{K}^e$	element stiffness matrix
$\mathbf{K}$	global stiffness matrix
$\mathbf{K}_D$	diagonal global stiffness matrix
$\mathbf{C}$	matrix containing the generalized eigenvectors
$\mathbf{f}^e(t)$	vector of element nodal forces
$\mathbf{h}^e(vt)$	analytic nodal force vector for a point load acting on element e
$\mathbf{h}(vt)$	global analytic force vector for a point load
$\mathbf{q}(t)$	time-dependent vector of modal amplitudes
ω_n	angular frequency of mode n
ζ_n	damping coefficient of mode n
ζ	constant damping coefficient

reported by two of its members, Frýba [1] and Mancel [2]. These authors pointed out that the occurrence of intense resonance phenomena associated with flexural oscillations needs further investigation.

Out of many alternatives used in the construction of road and railway bridges, one that is widespread is the simply supported beam or girder type of construction. With regard to this kind of structures, closed-form solutions for the moving load problem have been available since the beginning of the 20th century, see Bleich [3]. This type of solutions are generally in the form of an infinite series. A few terms would suffice for the computation of displacements because the series normally converges rapidly. However, the same does not apply to the evaluation of accelerations, bending moments and shear forces. Among recent publications related to the moving load problem in simply supported beams, the works of Frýba [4,5], Li and Su [6], Yang et al. [7], Gbadeyan and Oni [8], and Olsson [9] need special mention.

As for continuous beams, Hayashikawa and Watanabe [10] presented a closed-form solution by idealising the system as a stepped beam (i.e. a beam for which both the cross-sectional and the material properties are constant over intervals of finite length). The normal modes and natural frequencies were obtained by using the exact dynamic stiffness matrix. Subsequently, they used a Duhamel-type integration to solve the uncoupled modal equations. Chen and Li [11] obtained the exact modes from the dynamic stiffness matrix of a damped Timoshenko beam, and later expressed the equivalent modal loads in terms of complex exponential functions, thus leading to the closed-form solution of the governing equation in each mode directly. An approach in the frequency domain was proposed by Henchi et al. [12]. In this method the exact normal modes and natural frequencies were also obtained from the dynamic stiffness matrix, but then the modal equations were solved using the FFT algorithm. Nevertheless, as in the works of Hayashikawa and Watanabe [10] and Chen and Li [11], the approach was limited to the analysis of continuous stepped beams.

A more general method was developed by Dugush and Eisenberger [13], who expressed the normal modes as an infinite power series, and then computed the natural frequencies from the dynamic stiffness matrix using the method of bisection. The cross-sectional properties were assumed to follow polynomial variations. Subsequently, the governing differential equation of each mode was solved using an infinite power series expansion. Structural damping was not taken into account in the analysis.

Regarding closed-form solutions for continuous beams, the contribution of Cai et al. [14] should be mentioned. In this work the solution for an infinite continuous beam resting on periodic rollers and subjected to moving loads is obtained. By contrast, approximate solutions for continuous beams under moving forces have been developed by several authors. For example, Wu and Dai [15] proposed a method based on transfer matrices, Lee [16] used the assumed mode method and modelled the intermediate supports as very stiff springs and, more recently, Zheng et al. [17] presented a new approach based on modified beam vibration functions.

The methodology proposed in the present paper is semi-analytic. Its purpose is to analyse the flexural vibrations of the beam in the vertical plane, which is the one defined by the beam and the direction of the loads at any time. To this end, the beam is spatially discretized using the conventional finite elements with two nodes. Each node has two degrees of freedom: transverse displacement and rotation. Then, the (approximate) mode shapes and natural frequencies are computed using standard eigensolution procedure. Finally, the equivalent modal loads are expressed analytically in terms of the previously computed mode shapes. This leads to the mathematical expression of the time domain solution for each mode in a straightforward manner.

The approach presented in this paper provides an exact solution of the moving load problem in Bernoulli–Euler beams discretized with the usual two-noded finite elements with Hermitian shape functions. In addition, the formulation adopted herein allows for the use of non-uniform beam elements, for which the area and the second moment of area of the cross-section are assumed to follow linear and cubic variations, respectively. This is a valuable feature of the method, since a possible variation of the cross-sectional properties (which is usual in continuous bridges) can be represented more adequately by means of non-uniform elements than by a stepped discretization.

It should be emphasized that the proposed method, as will be shown later, is fast and robust, and therefore, circumvents the main disadvantages of the time-stepping schemes normally used in conjunction with the finite element method.

2. Formulation and semi-analytic solution

2.1. Weak and matrix formulations for a single element

Let $[0, L]$ be the domain of a Bernoulli–Euler non-uniform beam. The total length of the beam is L. Let $x \in [0, L]$ be the abscissa and $t \in [0, \infty)$ the time variable. The governing differential equation for a Bernoulli–Euler beam subjected to the action of a distributed load $p(x, t)$ and neglecting damping effects is given by

$$m(x)\frac{\partial^2 w(x,t)}{\partial t^2} + \frac{\partial^2}{\partial x^2}\left[\frac{\partial^2 w(x,t)}{\partial x^2} EI(x)\right] + p(x,t) = 0, \tag{1}$$

where $m(x)$ stands for the mass per unit length, E is the modulus of elasticity, and $I(x)$ is the variable second moment of area of the cross-section.

Fig. 1 shows the positive sign of the distributed load, shear force, and bending moment. The displacement function $w(x, t)$ is positive in the upward direction.

The single concentrated load traversing the beam at the constant speed v is idealized by means of Dirac Delta function $\delta(x)$. Thus, $p(x, t) = p_0\delta(x - vt)$ represents the effect of a concentrated load p_0. At this point,

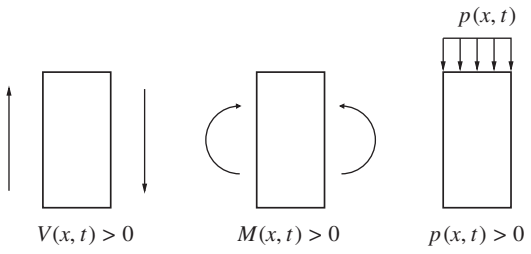

Fig. 1. Sign convention for the shear force, bending moment, and distributed load.

two time intervals are considered: $[0, L/v)$ or *forced vibrations*, when the load is acting upon the beam, and $[L/v, \infty)$ or *free vibrations*. During the forced vibration period, Eq. (1) can be rewritten as

$$m(x)\frac{\partial^2 w(x,t)}{\partial t^2} + \frac{\partial^2}{\partial x^2}\left[\frac{\partial^2 w(x,t)}{\partial x^2} EI(x)\right] + p_0\delta(x - vt) = 0. \tag{2}$$

The boundary conditions for this problem are

$$w(x,t)|_{t=0} = 0 \quad \forall x \in [0, L], \quad \left.\frac{\partial w(x,t)}{\partial t}\right|_{t=0} = 0 \quad \forall x \in [0, L]. \tag{3}$$

The weak formulation of the problem defined by Eq. (2) with the boundary conditions given in Eq. (3) is obtained by multiplying Eq. (2) by a generic test function $u^*(x)$ following a double integration by parts. Particularly, if a conventional finite element approach is adopted, the domain $x \in [0, L]$ is subdivided into elements of length l^e and Hermitian polynomials are used both as test functions as well as interpolating functions. Subsequently, the integration by parts of Eq. (2) is carried out over each element. This technique is widely known and is treated extensively in a number of works, see for instance the monograph by Bathe [18].

A typical beam finite element is shown in Fig. 2. Let i and j be the initial and end points or nodes. Also, let x_i^e and x_j^e be the abscissas corresponding to the extreme points, and x^e the abscissa relative to the origin of the element so that $x^e = x - x_i^e$. Positive nodal forces and moments are shown in Fig. 2.

In the local reference, the expressions of the four Hermitian polynomials $h_n^e(x), n = 1$ to 4, associated to element e are

$$\begin{aligned}
h_1^e(x^e) &= 1 - 3\left(\frac{x^e}{l^e}\right)^2 + 2\left(\frac{x^e}{l^e}\right)^3,\\
h_2^e(x^e) &= l^e\left[\frac{x^e}{l^e} - 2\left(\frac{x^e}{l^e}\right)^2 + \left(\frac{x^e}{l^e}\right)^3\right],\\
h_3^e(x^e) &= 3\left(\frac{x^e}{l^e}\right)^2 - 2\left(\frac{x^e}{l^e}\right)^3,\\
h_4^e(x^e) &= l^e\left[-\left(\frac{x^e}{l^e}\right)^2 + \left(\frac{x^e}{l^e}\right)^3\right].
\end{aligned} \tag{4}$$

Within the element, the function $w(x, t)$ is approximated by a cubic polynomial,

$$w(x^e, t) = \sum_{n=1}^{4} y_n^e(t) h_n^e(x^e), \tag{5}$$

where the physical meaning of the time-varying coefficients is the usual one, i.e. the transverse displacement and slope at the nodes

$$\begin{aligned}
y_1^e(t) &= y_i(t), \quad y_2^e(t) = \theta_i(t),\\
y_3^e(t) &= y_j(t), \quad y_4^e(t) = \theta_j(t).
\end{aligned} \tag{6}$$

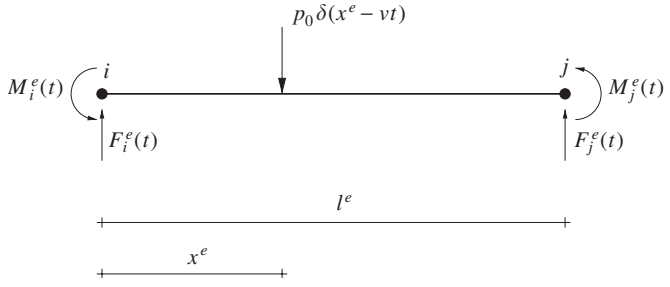

Fig. 2. Local reference for element e. Nodal forces and moments.

The approximate velocity and acceleration are obtained by differentiation of $w(x^e,t)$ with respect to time to give

$$\dot{w}(x^e,t)=\sum_{n=1}^{4}\dot{y}_n^e(t)h_n^e(x^e),\quad \ddot{w}(x^e,t)=\sum_{n=1}^{4}\ddot{y}_n^e(t)h_n^e(x^e), \tag{7}$$

where overdots denote time derivatives. Using the four Hermitian polynomials as test functions, and approximating the transverse displacement by means of Eq. (5), four equations are obtained from the weak form of Eq. (2)

$$\int_0^{l^e} m(x^e)\sum_{n=1}^{4}\{\ddot{y}_n^e(t)h_n^e(x^e)\}h_m^e(x^e)\,\mathrm{d}x^e+\int_0^{l^e}\sum_{n=1}^{4}\left\{y_n^e(t)\frac{\mathrm{d}^2h_n^e(x^e)}{\mathrm{d}(x^e)^2}\right\}EI(x^e)\frac{\mathrm{d}^2h_m^e(x^e)}{\mathrm{d}(x^e)^2}\,\mathrm{d}x^e$$
$$=F_j^e(t)h_m^e(l^e)+F_i^e(t)h_m^e(0)+M_j^e(t)\left.\frac{\mathrm{d}h_m^e(x^e)}{\mathrm{d}(x^e)}\right|_{l^e}+M_i^e(t)\left.\frac{\mathrm{d}h_m^e(x^e)}{\mathrm{d}(x^e)}\right|_0-p_0h_m^e(vt), \tag{8}$$

with $m=1$–4.

After evaluation of the integrals contained in Eqs. (8), the solution can be conveniently arranged in matrix form. For element e, the following linear relationship is obtained:

$$\begin{pmatrix} m_{11}^e & m_{12}^e & m_{13}^e & m_{14}^e\\ m_{21}^e & m_{22}^e & m_{23}^e & m_{24}^e\\ m_{31}^e & m_{32}^e & m_{33}^e & m_{34}^e\\ m_{41}^e & m_{42}^e & m_{43}^e & m_{44}^e\end{pmatrix}\begin{pmatrix}\ddot{y}_i(t)\\ \ddot{\theta}_i(t)\\ \ddot{y}_j(t)\\ \ddot{\theta}_j(t)\end{pmatrix}+\begin{pmatrix} k_{11}^e & k_{12}^e & k_{13}^e & k_{14}^e\\ k_{21}^e & k_{22}^e & k_{23}^e & k_{24}^e\\ k_{31}^e & k_{32}^e & k_{33}^e & k_{34}^e\\ k_{41}^e & k_{42}^e & k_{43}^e & k_{44}^e\end{pmatrix}\begin{pmatrix}y_i(t)\\ \theta_i(t)\\ y_j(t)\\ \theta_j(t)\end{pmatrix}$$
$$=\begin{pmatrix}F_i^e(t)\\ M_i^e(t)\\ F_j^e(t)\\ M_j^e(t)\end{pmatrix}-p_0\begin{pmatrix}h_1^e(vt)\\ h_2^e(vt)\\ h_3^e(vt)\\ h_4^e(vt)\end{pmatrix}, \tag{9}$$

which can also be rewritten in a more compact form as

$$\mathbf{M}^e\ddot{\mathbf{y}}^e(t)+\mathbf{K}^e\mathbf{y}(t)=\mathbf{f}^e(t)-p_0\mathbf{h}^e(vt). \tag{10}$$

The elements of the matrices in Eq. (9) are given by the usual expressions

$$m_{rs}^e=\int_0^{l^e}m(x^e)h_r^e(x^e)h_s^e(x^e)\,\mathrm{d}x^e,$$
$$k_{rs}^e=\int_0^{l^e}\frac{\mathrm{d}^2h_r^e(x^e)}{\mathrm{d}(x^e)^2}EI(x^e)\frac{\mathrm{d}^2h_s^e(x^e)}{\mathrm{d}(x^e)^2}\,\mathrm{d}x^e, \tag{11}$$

where r and s run from 1 to 4.

At this point, it should be emphasized that the term $\mathbf{h}^e(vt)$ in Eq. (10) is the analytic expression of the unit load vector for element e.

2.2. Interpolation of the mass per unit length and second moment of area

Different alternatives can be adopted for interpolating the mass per unit length $m(x)$ and second moment of area $I(x)$ along the length of an element. In this paper it is assumed that the cross-section of the element is rectangular. Linear variations of the area and the depth of the section are assumed, leading to a linear variation of the mass per unit length, and a cubic variation of the second moment of area of the cross-section.

This kind of interpolation proves particularly convenient for applications in bridge design, where $m(x)$ and $I(x)$ are defined from the values at the extremes of the element. This is of considerable interest because it allows possible discontinuities in both functions. Nonetheless, other different variations can be assumed

without loosing the generality of the approach. The variations of the mass per unit length and the second moment of area are defined as follows:

- *Mass per unit length*:
  Let ρ be the volumetric mass density. The total mass per unit length corresponding to a section consists of two terms: the mass associated with the self-weight and a permanent added mass which proves useful for practical applications. Accordingly, the function $m(x^e)$ is

$$m(x^e) = \rho A_i^e + \rho \frac{A_j^e - A_i^e}{l^e} x^e + \gamma, \tag{12}$$

  where A_i^e is the area of the cross-section at node i of element e (*initial* area), A_j^e the area of the cross-section at node j of element e (*final* area) and γ the permanent mass added to the self-weight of the beam.
  Eq. (12) can be rewritten more simply if the masses per unit length at the nodes are introduced:

$$m_i^e = \rho A_i^e + \gamma, \quad m_j^e = \rho A_j^e + \gamma. \tag{13}$$

  Thus,

$$m(x^e) = m_i^e + \frac{m_j^e - m_i^e}{l^e} x^e. \tag{14}$$

- *Second moment of area of the cross-section*
  Now a cubic interpolation for the second moment of area of the cross-section is presented here. The interpolation is based on the use of equivalent rectangular sections. For a rectangular section, the second moment of area can be expressed in terms of the area and the depth of the beam as follows:

$$I(x) = \tfrac{1}{12} A(x)\, d^2(x), \tag{15}$$

  where d is the depth of the section.
  The equivalent rectangular sections corresponding to the nodes i and j of element e can be derived from the actual area and second moment of area using Eq. (15). Thus, the depth of these equivalent sections is

$$d_i^e = \sqrt{\frac{12 I_i^e}{A_i^e}}, \quad d_j^e = \sqrt{\frac{12 I_j^e}{A_j^e}}. \tag{16}$$

  Subsequently, linear variations of the area and the equivalent depth over the length of the element are assumed to be

$$A(x^e) = A_i^e + \frac{A_j^e - A_i^e}{l^e} x^e, \quad d(x^e) = d_i^e + \frac{d_j^e - d_i^e}{l^e} x^e. \tag{17}$$

  Finally, substituting Eq. (17) into Eq. (15), a cubic variation of second moment of area along the length of the element is obtained. The expressions of the element mass and stiffness matrix resulting from the above property variations are shown in Appendix A.

2.3. Assembled formulation

Assembling the element equations (10) in the usual form, the differential equation of motion of the finite element model of the beam is obtained as

$$\mathbf{M}\ddot{\mathbf{y}}(t) + \mathbf{K}\mathbf{y}(t) = -p_0 \mathbf{h}(vt). \tag{18}$$

It can be seen, the load term is a vector with an analytic, polynomial expression for $t \in [x_i^e/v, x_j^e/v)$. In what follows it will be assumed that the load has moved to the next element when $t = x_j^e/v$, and therefore, the right end of the interval is excluded.

In order to solve Eq. (18), the boundary conditions need to be prescribed. The simply supported boundary condition is the most usual one in the analysis of multi-span beams, but others are also possible in practice,

such as both ends fixed or cantilever. After applying the boundary conditions, the new reduced mass and stiffness matrices define the problem to be solved. For simplicity, in what follows the reduced matrices will be referred to using the same symbols as the non-reduced ones, and distinction will be made when it is necessary.

3. Solution of the equations of motion

Eq. (18) is a matrix system of linear differential equations with constant coefficients and an analytic right-hand term (load vector) for each time interval $[x_i^e/v, x_j^e/v)$. After applying the boundary conditions, this equation can be solved through a change of basis. The new basis is given by the generalized eigenvalue problem described by

$$(-\omega^2\mathbf{M}+\mathbf{K})\mathbf{y}(t)=0 \Rightarrow |\mathbf{K}-\omega^2\mathbf{M}|=0 \tag{19}$$

ω being the generalized eigenvalue. Let $\mathbf{q}(t)$ be the time-dependent modal amplitude vector, related to $\mathbf{y}(t)$ through the matrix $\mathbf{C}$ as follows:

$$\mathbf{y}(t)=\mathbf{C}\mathbf{q}(t), \tag{20}$$

where each column of $\mathbf{C}$ contains the corresponding generalized eigenvector. Premultiplying Eq. (18) by $\mathbf{C}^{\mathrm{T}}$ and changing from $\mathbf{y}(t)$ to $\mathbf{q}(t)$ one obtains

$$\mathbf{C}^{\mathrm{T}}\mathbf{M}\mathbf{C}\ddot{\mathbf{q}}(t)+\mathbf{C}^{\mathrm{T}}\mathbf{K}\mathbf{C}\mathbf{q}(t)=-p_0\mathbf{C}^{\mathrm{T}}\mathbf{h}(vt). \tag{21}$$

As it is known, the matrix products in the left-hand terms of Eq. (21) are diagonal as a result of the orthogonality property of the modes. Therefore, Eq. (21) becomes

$$\mathbf{M}_D\ddot{\mathbf{q}}(t)+\mathbf{K}_D\mathbf{q}(t)=-p_0\mathbf{C}^{\mathrm{T}}\mathbf{h}(vt). \tag{22}$$

The problem can now be solved for a unitary load, $p_0=1$ and, assuming linear behaviour of the system, the solution for a different load can be computed multiplying the unitary solution by the actual value of p_0. Premultiplying Eq. (22) by the inverse of the diagonal mass matrix, and letting $p_0=1$ yields

$$\ddot{\mathbf{q}}(t)+\mathbf{M}_D^{-1}\mathbf{K}_D\mathbf{q}(t)=\mathbf{G}\mathbf{h}(vt), \tag{23}$$

where

$$\mathbf{G}=-\mathbf{M}_D^{-1}\mathbf{C}^{\mathrm{T}}. \tag{24}$$

With the exception of the time intervals when the load is applied in one element having a restrained degree of freedom, the elements of vector $\mathbf{h}(vt)$ in the right-hand term of Eq. (23) are zero in all but four rows. These four rows correspond precisely to the degrees of freedom of the nodes i,j belonging to the element e where the moving load is applied. Thus, the differential equation for the nth mode can be expressed as

$$\ddot{q}_n(t)+\omega_n^2 q_n(t)=\sum_{m=1}^{4} G_{nm}^e h_m^e(vt), \tag{25}$$

where ω_n is the frequency of the nth mode, G_{nm}^e represent the coefficients of the nth row of matrix $\mathbf{G}$ corresponding to element e, and the mth Hermitian function of the element; such Hermitian function is represented by h_m^e.

If the existing boundary conditions eliminate a certain degree of freedom of the load vector, a zero value is given to the appropriate coefficient G_{nm}^e, thus preserving the generality of the approach.

At this point it is possible to include the damping effects by means of a modal damping ratio ζ_n (the damping ratios for each mode are usually computed from experimental tests carried out in real structures). In this way Eq. (25) transforms into

$$\ddot{q}_n(t)+2\zeta_n\omega_n\dot{q}_n(t)+\omega_n^2 q_n(t)=\sum_{m=1}^{4} G_{nm}^e h_m^e(vt). \tag{26}$$

The solution of Eq. (26) can be obtained in closed-form, but the analytic expression needs to be defined piecewise for every different time interval $[x_i^e/v,\ x_j^e/v)$. Every time the load crosses from one element to the next one, the closed-form expression of the solution is redefined.

Consider that the load is moving in element e, having initial and final nodes i and j. In order to solve Eq. (26), a change of the origin of the time variable is introduced. Let τ be the time relative to the instant when the load passes over the initial node i ($\tau = t - x_i^e/v$). Then, the initial conditions can be specified in the form

$$q_n(\tau = 0) = q_n^0, \quad \dot{q}_n(\tau = 0) = \dot{q}_n^0, \tag{27}$$

with $\tau \in [0, l^e/v)$.

The solution can now be obtained adding the solution of the homogeneous equation *plus* a particular solution

$$q_n(\tau) = q_n^h(\tau) + q_n^p(\tau). \tag{28}$$

The mathematical expressions of these solutions are the following:

$$q_n^h(\tau) = \mathrm{e}^{-\zeta_n\omega_n\tau}(A_n\cos(\omega_n^d\tau) + B_n\sin(\omega_n^d\tau)), \tag{29}$$

where

$$\omega_n^d = \sqrt{1-(\zeta_n)^2} \tag{30}$$

and

$$q_n^p(\tau) = \alpha_n^{(0)} + \alpha_n^{(1)}v\tau + \alpha_n^{(2)}(v\tau)^2 + \alpha_n^{(3)}(v\tau)^3. \tag{31}$$

Coefficients $\alpha_n^{(0)}, \alpha_n^{(1)}, \alpha_n^{(2)}, \alpha_n^{(3)}$ can be obtained from the expressions below:

$$\begin{aligned}
\alpha_n^{(0)} &= v^3\alpha_n^{(01)} + v^2\alpha_n^{(02)} + v\alpha_n^{(03)} + \alpha_n^{(04)},\\
\alpha_n^{(1)} &= v^2\alpha_n^{(11)} + v\alpha_n^{(12)} + \alpha_n^{(13)},\\
\alpha_n^{(2)} &= v\alpha_n^{(21)} + \alpha_n^{(22)},\\
\alpha_n^{(3)} &= \alpha_n^{(31)}.
\end{aligned} \tag{32}$$

In the above expressions, the dependence of the speed v has been isolated using the following 10 coefficients:

$$\alpha_n^{(01)} = -\frac{24\zeta_n(2(\zeta_n)^2-1)(2G_{n1}^e - 2G_{n3}^e + (G_{n2}^e + G_{n4}^e)l^e)}{(l^e)^3(\omega_n)^5},$$

$$\alpha_n^{(02)} = -\frac{2(4(\zeta_n)^2-1)(3G_{n1}^e - 3G_{n3}^e + (2G_{n2}^e + G_{n4}^e)l^e)}{(l^e)^2(\omega_n)^4},$$

$$\alpha_n^{(03)} = -\frac{2G_{n2}^e\zeta_n}{(\omega_n)^3},$$

$$\alpha_n^{(04)} = \frac{G_{n1}^e}{(\omega_n)^2},$$

$$\alpha_n^{(11)} = \frac{6(4(\zeta_n)^2-1)(2G_{n1}^e - 2G_{n3}^e + (G_{n2}^e + G_{n4}^e)l^e)}{(l^e)^3(\omega_n)^4},$$

$$\alpha_n^{(12)} = \frac{4\zeta_n(3G_{n1}^e - 3G_{n3}^e + (2G_{n2}^e + G_{n4}^e)l^e}{(l^e)^2(\omega_n)^3},$$

$$\alpha_n^{(13)} = \frac{G_{n2}^e}{(\omega_n)^2},$$

$$\alpha_n^{(21)} = -\frac{6\zeta_n(2G_{n1}^e - 2G_{n3}^e + (G_{n2}^e + G_{n4}^e)l^e)}{(l^e)^3(\omega_n)^3},$$

$$\alpha_n^{(22)} = -\frac{3G_{n1}^e - 3G_{n3}^e + (2G_{n2}^e + G_{n4}^e)l^e}{(l^e)^2(\omega_n)^2},$$
$$\alpha_n^{(31)} = \frac{2G_{n1}^e - 2G_{n3}^e + (G_{n2}^e + G_{n4}^e)l^e}{(l^e)^3(\omega_n)^2}. \tag{33}$$

The coefficients can now be computed and stored initially for the entire mesh. For a given speed of the moving load, the coefficients of the particular solution are computed for each element using Eq. (32). The coefficients of the homogeneous solution (29) are obtained from the initial conditions (27) as follows:

$$A_n = q_n^0 - \alpha_n^0,$$
$$B_n = \frac{\dot{q}_n^0 + \zeta_n\omega_n A_n - \alpha_n^{(1)}v}{\omega_n^d}. \tag{34}$$

So, the complete closed-form solution is built piecewise from a set of analytic functions, one per element. For the initial time, $t = 0$, at-rest conditions are normally imposed:

$$q_n(\tau = 0) = 0, \quad \dot{q}_n(\tau = 0) = 0. \tag{35}$$

For the following elements, the initial conditions for element $e + 1$ are given by the end values of element e. Thus

$$q_n(\tau)|_{\tau=0}^{e+1} = q_n(\tau)|_{\tau=l^e/v}^{e},$$
$$\dot{q}_n(\tau)|_{\tau=0}^{e+1} = \dot{q}_n(\tau)|_{\tau=l^e/v}^{e}. \tag{36}$$

During the time interval in which the load traverses the structure, the particular and homogeneous solutions will have to be added, giving rise to the forced vibration and free vibration contributions, respectively. Conversely, after the load has reached the last node of the beam only the contribution of the homogeneous solution will remain.

Two aspects are remarkable at this point. First, in Eq. (29) the introduction of the local time τ leads to bounded exponential terms, which is crucial for computational purposes. This is a well-known problem: despite existing analytic solutions for some cases of single or multispan beams, a spatial mesh must be introduced in order to avoid numerical problems with exponential terms. Secondly, Eqs. (36) entail that the modal amplitudes q_n and their derivatives are continuous, even if they are defined piecewise; considering that the load term in Eq. (26) is also continuous because it represents the modal shape multiplied by the load, it can be concluded that a continuous modal acceleration is obtained from the semi-analytic procedure presented in this paper.

4. Solution for a set of moving loads

For a set or series of concentrated loads moving at a constant speed v, the solution can be obtained by superposition. One of the most demanding situations from a computational point of view is the parametric analysis of a beam over a wide range of speeds; in addition, real trains usually present a large number of loads whose effects have to be superimposed. In this regard, the solution proposed herein demonstrates three main characteristics:

- It is easy to store, say, 10 coefficients per element and per mode.
- The closed-form expressions are computed accurately.
- It is easily adaptable for different speeds of the train.

For computing purposes, the solution presented in Section 3 can be stored in two steps:

(1) Ten coefficients per element and per mode given by Eqs. (33). These coefficients do not depend on the speed, so they can be stored initially for the entire mesh and for all the modes considered in the analysis.
(2) For any given speed, the coefficients of the particular solution ($\alpha_n^{(0)}$, $\alpha_n^{(1)}$, $\alpha_n^{(2)}$ and $\alpha_n^{(3)}$) and of the homogeneous equation (A_n and B_n) are calculated and stored for each mode and element.

At a fixed time, the loads that contribute to the response of the beam are those acting upon the structure and those that already have left it. The computation of the contributions of the loads that are travelling over the structure requires a fixed number of floating point operations per load. On the contrary, for the ensemble of loads that have left the beam it proves to be more convenient to gather all their contributions in a unique damped sinusoidal function, similar to Eq. (29). This can be done by updating the coefficients of this function for each mode, say A_n and B_n, every time a new load abandons the structure.

5. Numerical tests

In this section a set of numerical results is presented for illustration purposes to demonstrate the semi-analytic approach proposed in this paper.

Sections 5.1–5.3 show three different comparisons of the results obtained using the semi-analytic method and a classic time-stepping procedure: the linear acceleration version of the Newmark method.

The linear acceleration method has been selected for the resolution of the differential modal equations for two main reasons. First, because it is a well-known method that serves as a basis for the validation of the new methodology proposed herein. Secondly, because it provides a useful means of emphasizing that the semi-analytic approach cannot be affected by any numerical integration error, as the examples below will clearly illustrate.

Finally, Section 5.4 presents a practical application of the semi-analytic method to the dynamic analysis of a three-span bridge according to Eurocode 1 [19].

For all the examples, a constant damping ratio for all modes has been assumed, so that $\zeta_n = \zeta$.

5.1. A three-span continuous stepped beam under a single moving load

Fig. 3 shows a three-span beam considered as an example. This example has been used by Hayashikawa and Watanabe [10], Henchi et al. [12], and Zheng et al. [17]. The length of each span is 20 m. The mass per unit length (ρA) is 1000 kg/m, and it is constant for all spans. The flexural stiffness EI is 1.96 GN m^2 for the end spans, whereas the stiffness of the central span is twice this value. The damping coefficient ζ is set to zero. The beam is subjected to the action of a single load of 9.8 kN. The constant speed of the load is assumed to be 35.57 m/s. Each span has been divided into 10 elements of equal length, so that the total number of elements is 30. The number of modes considered in the analysis is 12; the natural frequencies are listed in Table 1.

The aim of this test is to compare the results obtained with the semi-analytic approach and the ones obtained using a step-by-step method for the case with no damping. Different analyses have been performed with the Newmark method considering various time steps, and the effects of the step size on the computed displacements and accelerations have been analysed. The time step used in each analysis is expressed as a fraction of the minimum period T_{12} (i.e. the period of the 12th mode).

Fig. 4 shows the acceleration obtained using the semi-analytic solution sampled at $T_{12}/10$. In the same plot the acceleration obtained with the Newmark method considering two different time steps is also shown: $T_{12}/25$ and $T_{12}/150$ have been used. Only the beginning of the time-histories is shown in the figure. As can be seen, very good agreement is found between the three curves.

On the contrary, if one examines the time-histories after some seconds have passed, differences arising from numerical integration errors can be found. This is shown in Fig. 5. Note that still very good agreement is found between the semi-analytic solution and the Newmark method for the case with $T_{12}/150$. By contrast, the results corresponding to $T_{12}/25$ are visibly different. This is largely a consequence of the period elongation error inherent to the linear acceleration method.

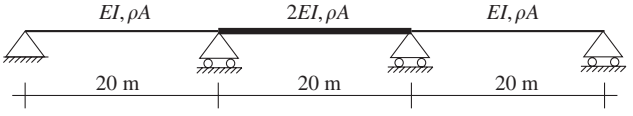

Fig. 3. A three-span continuous stepped beam.

Table 1
Natural frequencies (v_j) for the three-span continuous stepped beam

j	v_j (Hz)
1	6.2043
2	7.5812
3	11.9743
4	24.2102
5	26.4434
6	37.2897
7	53.6117
8	56.6805
9	77.0261
10	94.3304
11	98.7615
12	130.7492

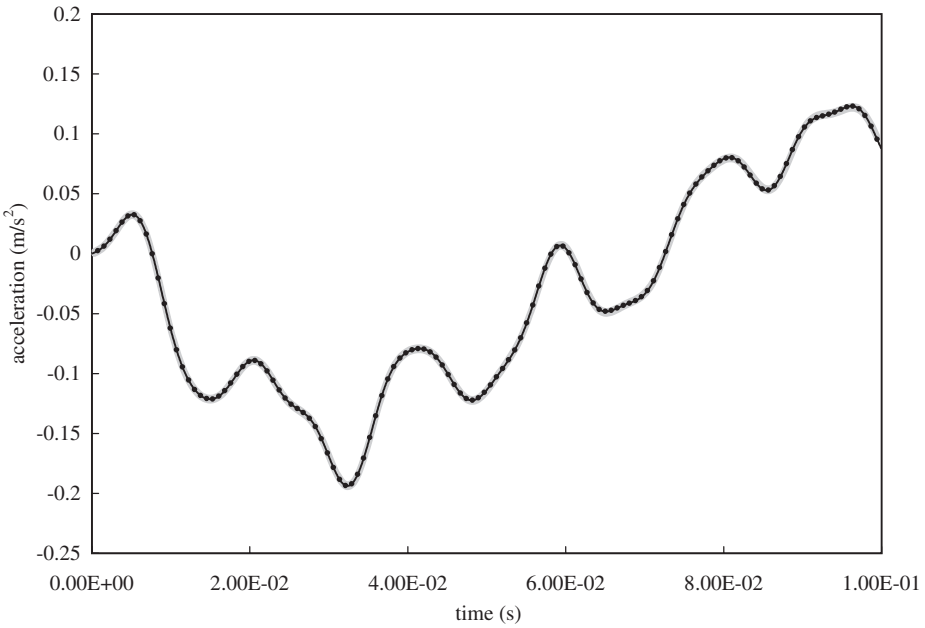

Fig. 4. Acceleration at the mid-span section of the left span for a stepped beam subjected to a moving load: $0 \leqslant t \leqslant 0.1$. • Semi-analytic ($T_{12}/10$); —— Newmark ($T_{12}/25$); —— Newmark ($T_{12}/150$).

The use of more sophisticated numerical schemes is expected to give more accurate results for $T_{12}/25$ or even longer time steps. However, as stated before, the choice of the Newmark method is adequate for the purpose of this comparison (other suitable methods could have been used also). Specifically, this purpose is to highlight that, at any fixed time instant, the response computed using the semi-analytic approach is independent of the time step; the time step is used only for *evaluating* the response, but it is not related to the integration of the equations of motion. When compared with any approximated method, this entails a great advantage in terms of accuracy and robustness.

Finally, Fig. 6 shows the displacement computed at the mid-span section of the left span. In this case the semi-analytic solution is evaluated using a step equal to T_{12}, while the integration step used in the Newmark method is $T_{12}/25$. Excellent agreement is observed. Though not shown in the figure for the sake of clarity, such agreement is maintained for a long interval; the reason for this is that higher modes have generally

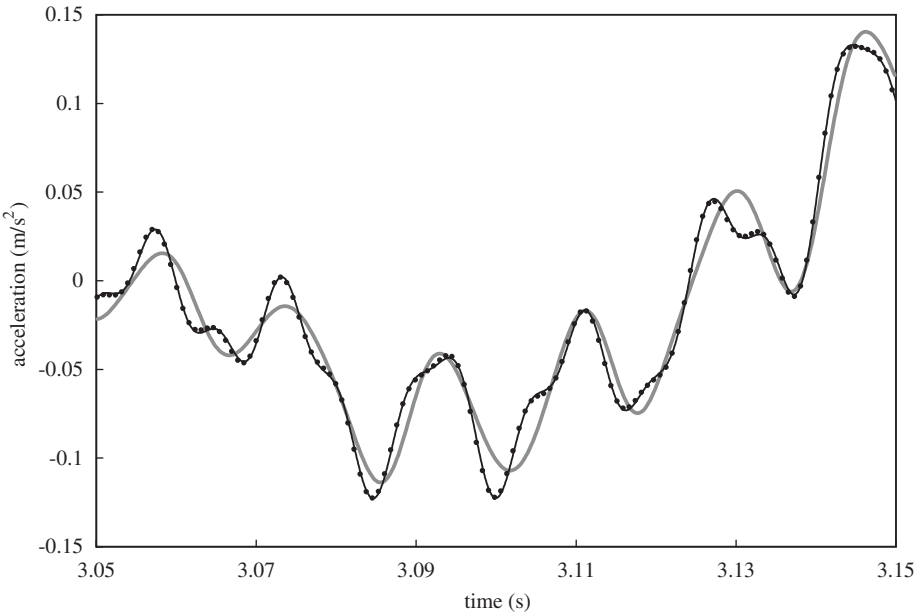

Fig. 5. Acceleration at the mid-span section of the left span for a stepped beam subjected to a moving load: $3.05 \leqslant t \leqslant 3.15$. • Semi-analytic ($T_{12}/10$); —— Newmark ($T_{12}/25$); —— Newmark ($T_{12}/150$).

negligible influence on the overall displacement, and therefore, the integration errors alter slightly the values predicted for this magnitude.

5.2. A three-span continuous haunched beam under a single moving load

In order to demonstrate the capabilities of the semi-analytic solution for the analysis of beams with variable cross-section, the response of the three-span haunched girder shown in Fig. 7 is analysed. The length of each end span is 18 m, whereas the length of the central span is 24 m. A linear variation of the depth is defined in the sections close to the intermediate supports. The density ρ is 2400 kg/m^3. The Young's modulus E is 30 000 MPa. The damping coefficient ζ is 1%, and a single load value of 9.8 kN, travelling at a speed of 100 m/s, has been considered.

A symmetric mesh has been used. Each end span is divided into 10 elements as follows: the first 6 m (beginning from the end support) are divided into three elements; the linear transition close to the intermediate support is also divided into three elements; the remaining 6 m are divided into four elements. The central span is meshed using 14 elements as follows: each linear transition is meshed with three elements, while the central uniform section is meshed with eight elements.

Twelve modes have been considered; the natural frequencies are listed in Table 2. The displacement and acceleration time-histories at the mid-span section of the left span have been obtained with the Newmark method and the semi-analytic solution. The time step used in the Newmark method is $T_{12}/25$, T_{12} being the period of the 12th mode. As regards the semi-analytic solution, T_{12} have been used for evaluating the displacement shown in Fig. 8 and the acceleration shown in Fig. 10. In Fig. 9 $T_{12}/5$ has been used in order to visualize correctly the high-frequency accelerations. As it can be observed, very good agreement is achieved in all cases.

Since structural damping has been included ($\zeta = 0.01$ for all modes), a time step equal to $T_{12}/25$ proves enough to obtain highly accurate results using the Newmark method. The reason is apparent from Figs. 9 and 10: the higher modes, which are more likely to suffer from numerical integration errors, are damped out after a certain time, and therefore their influence on the response diminishes (as can be observed, the high-frequency content present in Fig. 9 has almost disappeared in Fig. 10). One last example of the influence of damping on numerical integration errors is shown in Section 5.3.

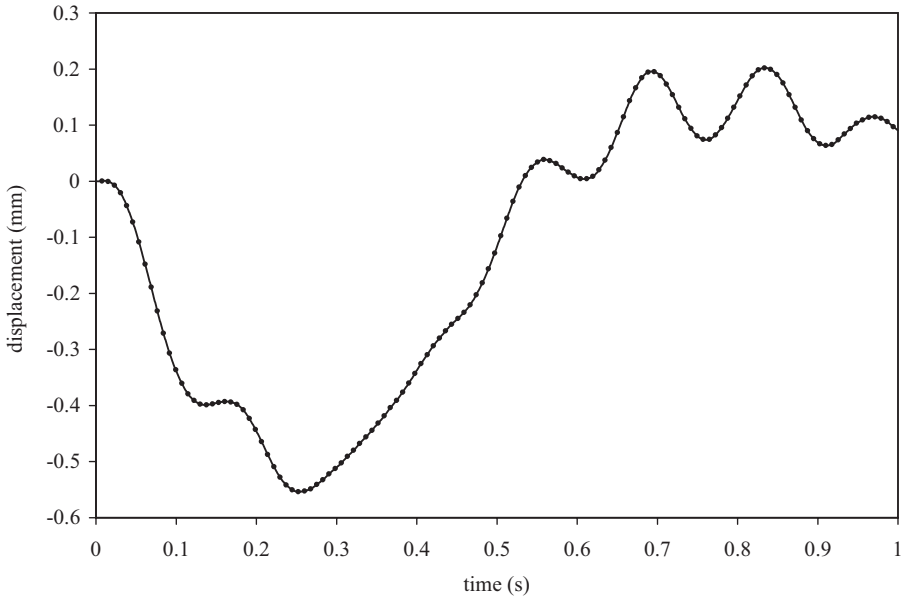

Fig. 6. Displacement at the mid-span section of the left span for a stepped beam subjected to a moving load. • Semi-analytic ($T_{12}/10$); —— Newmark ($T_{12}/25$).

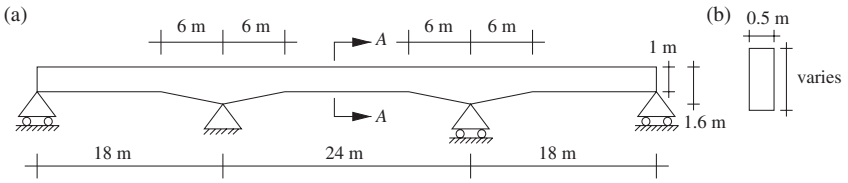

Fig. 7. A three-span continuous non-uniform beam: (a) elevation; (b) section *A–A*.

Table 2
Natural frequencies (v_j) for the three-span continuous haunched beam

j	v_j (Hz)
1	3.9200
2	6.6592
3	9.2386
4	15.8294
5	22.9459
6	26.4045
7	35.1403
8	48.9991
9	53.8260
10	62.0935
11	82.5022
12	91.7342

5.3. A three-span continuous haunched beam under a train of moving loads

In this section the response of the haunched beam defined in Section 5.2 subjected to a train of moving loads is analysed. Two different damping ratios have been considered. These are 0.5% and 3%. In this case only the

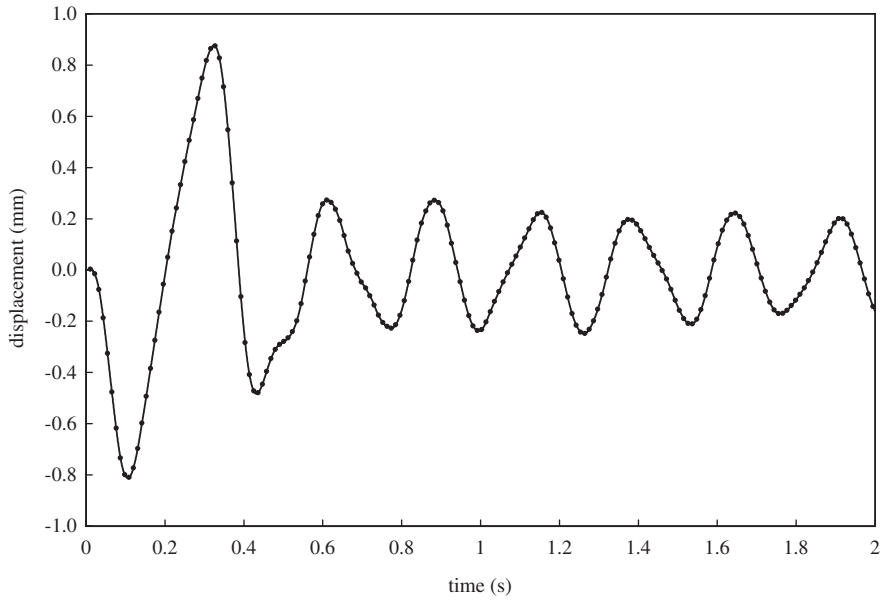

Fig. 8. Displacement at the mid-span section of the left span of a haunched beam. • Semi-analytic (T_{12}); —— Newmark ($T_{12}/25$).

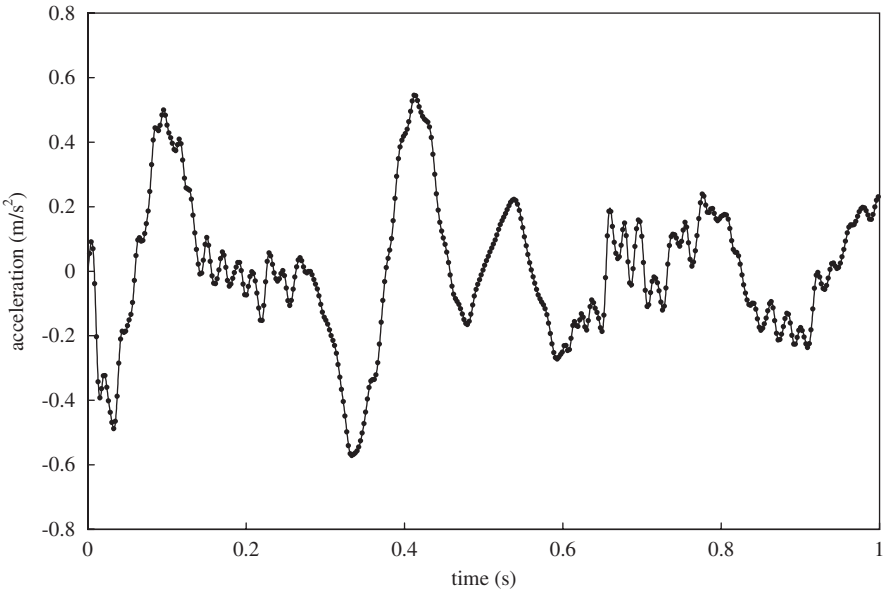

Fig. 9. Acceleration at the mid-span section of the left span of a haunched beam: $0 \leqslant t \leqslant 1$. • Semi-analytic ($T_{12}/5$); —— Newmark ($T_{12}/25$).

contributions of the first six modes of vibration have been taken into account. The train passing over the bridge consists of five equally spaced loads. The value of each load is 10 kN, and the distance between any two consecutive loads is 25 m. The speed of the train is 70 m/s. The response in terms of vertical acceleration has been computed at the mid-span section of the central span, and the corresponding time-histories are shown in Figs. 11 and 12.

Fig. 11 shows the accelerations corresponding to a damping ratio equal to 3%. The time step used in the Newmark method is $T_6/10$. The semi-analytic solution is sampled using the same step. The irregularity of the

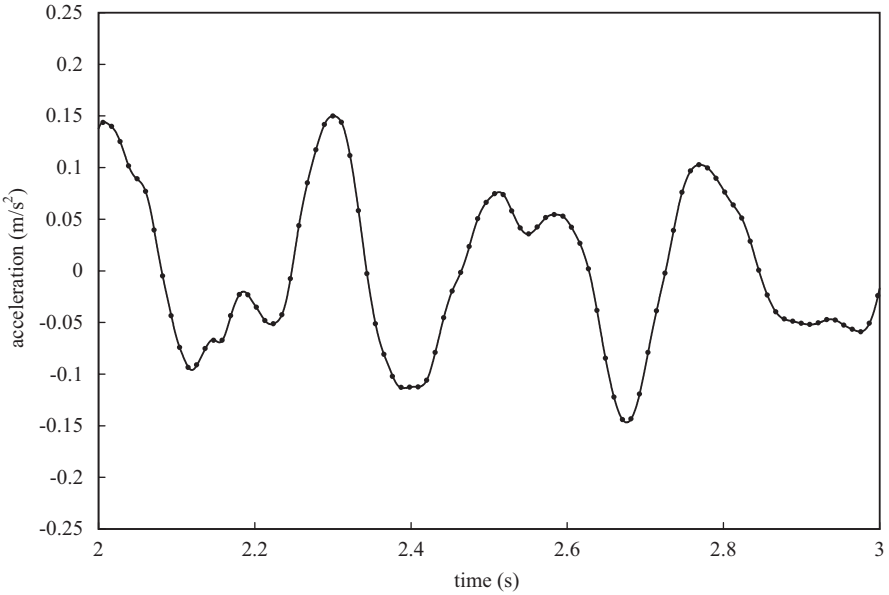

Fig. 10. Acceleration at the mid-span section of the left span of a haunched beam: $2 \leqslant t \leqslant 3$. • Semi-analytic ($T_{12}$); —— Newmark ($T_{12}/25$).

curve denotes the influence of higher modes. Nevertheless, an acceptable agreement is obtained between the semi-analytic and the numerical solution despite of the use of such a long integration step.

At this point it is important to stress that the cause of such a good agreement is damping, as Fig. 12 reveals. The only difference between the results presented in Fig. 11 and the ones in Fig. 12 is that the former correspond to 3% damping while the latter correspond to 0.5%. When a low damping ratio such as 0.5% is used, a long time is required before the influence of higher modes vanishes, and therefore numerical errors arising from the use of a long integration step are likely to spoil the solution. This kind of behaviour is precisely what Fig. 12 shows.

5.4. Dynamic analysis of a three-span bridge according to Eurocode 1

The purpose of this example is to illustrate one of the most relevant applications of the semi-analytic method presented in this paper: the dynamic analysis of high-speed railway bridges.

The last draft of Eurocode 1 [19] states that a dynamic analysis has to be carried out if a continuous bridge is to be traversed by high-speed trains. Bridges situated in international lines where European interoperability criteria are applicable must fulfil some particular requirements; specifically, a dynamic analysis of the bridge subjected to the action of 10 high-speed trains defined in Eurocode 1 ought to be undertaken. The ensemble of these 10 trains is the High-Speed Load Model, abbreviated through the text of the mentioned code as HSLM.

The bridge considered in this example is a real three-span, high-speed bridge carrying only one track (actually, the complete structure is formed by two adjacent single-track bridges allowing for the passage of two trains circulating in opposite directions). The structure is similar to the one shown in Fig. 3, but in this case the length of the end spans is 25 m and the central span is 38 m long. Also, the cross-sectional properties are constant along the bridge: the mass per unit length (ρA) is 14435.25 kg/m, the flexural stiffness EI is 110649.6 MN m^2, and a damping ratio ζ equal to 1% has been considered. The bridge is designed for an operating speed of 350 km/h; therefore, according to Eurocode 1, it must be analysed under the action of the HSLM model at speeds ranging from 40 m/s to a maximum of 117 m/s (approximately equal to $1.2 \times 350 = 420$ km/h). Steps of 1 m/s have been used in the analysis. As regards the Finite Element model, each span has been divided into 10 elements of equal length.

The contributions of the first five modes have been considered; this ensures that accelerations up to 30 Hz are correctly accounted for, as the Annex 2 of the basic Eurocode [20] imposes. Besides, it has been confirmed

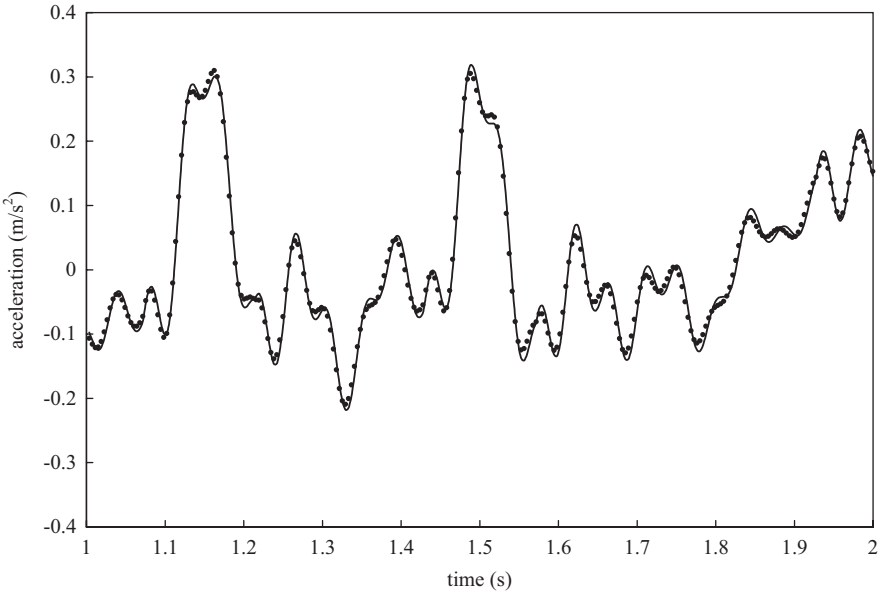

Fig. 11. Acceleration at the mid-span section of the central span of a haunched beam under a train of moving loads. 3% damping. • Semi-analytic ($T_6/10$); —— Newmark ($T_6/10$).

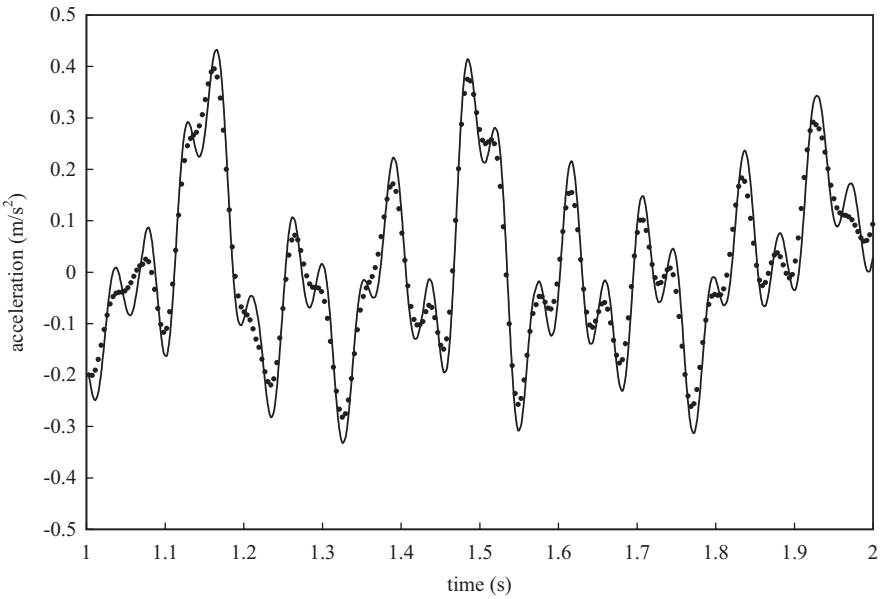

Fig. 12. Acceleration at the mid-span section of the central span of a haunched beam under a train of moving loads. 0.5% damping.• Semi-analytic ($T_6/10$); —— Newmark ($T_6/10$).

that in this case the contribution of higher modes to the maximum displacement is negligible. The natural frequencies of the bridge are listed in Table 3. The time step used for evaluating the response was 0.003 s.

During an actual design process the maximum vertical acceleration and maximum vertical displacement in several sections of the deck have to be computed for the verification of the Serviceability Limit States. Fig. 13 shows the maximum acceleration at the mid-span section of the central span, one of the most representative locations along the bridge. The results are presented as a function of the speed. The maximum acceleration has

Table 3
Natural frequencies (v_j) for the three-span continuous beam

j	v_j (Hz)
1	4.2806
2	8.1957
3	9.5925
4	15.8221
5	27.5136

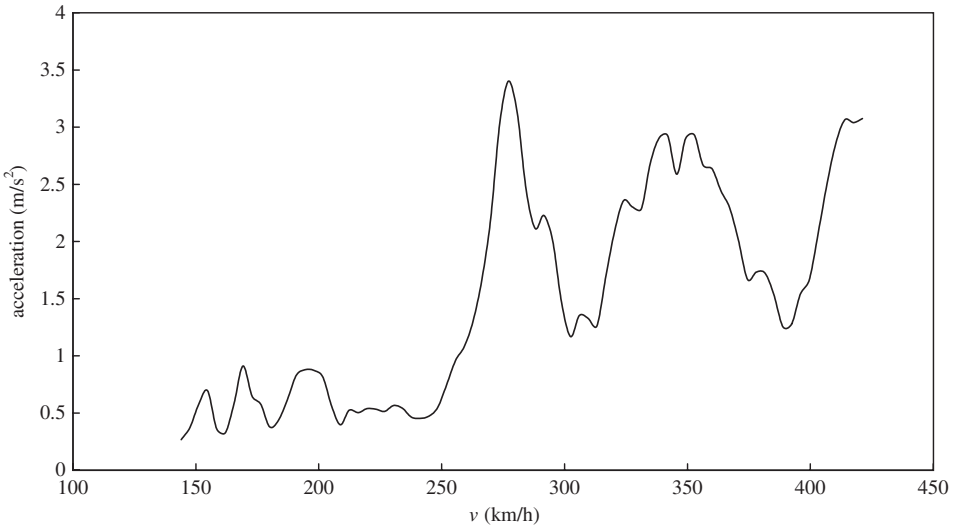

Fig. 13. A three-span continuous bridge subjected to the 10 high-speed trains defined in Eurocode 1. Envelope of the absolute values of the maximum accelerations at the mid-span section of the central span.

been computed for the 10 trains comprised in the HSLM, but only the envelope curve has been depicted. The maximum value permitted by the Annex 2 of the basic Eurocode [20], considering that the bridge carries a ballasted track, is 3.5 m/s^2. As it can be observed, in the central section of the bridge the response does not exceed this limit.

Attention should be drawn to the elevated number of time-history analyses that must be carried out in order to complete the dynamic analysis of the bridge. In this example 10 trains and 78 different values of speed have been considered, which gives a total of 780 time-history analysis. Moreover, these 780 analyses will probably have to be repeated several times during the design process until the engineer finds a satisfactory solution for the bridge. Therefore, it is essential for the structural engineer involved in the dynamic assessment of high-speed bridges to have at his/her disposal a fast and reliable method. The reliability and robustness of the semi-analytic solution proposed in this paper has been illustrated in the preceding sections. Besides, this has also proved to be a very fast method: the CPU time required for completing the 780 analysis was 23.39 s in a standard PC equipped with an AMD Athlon XP 2000 processor and a DDR 266 MHz RAM memory.

6. Summary

A semi-analytic solution for the moving load problem in multi-span non-uniform Bernoulli–Euler beams has been presented. The salient features of this methodology are:

(1) The time-dependent modal equations are solved in closed-form, and therefore, the method is highly accurate and robust, circumventing the main disadvantages of time-stepping schemes. The solution is

obtained in terms of 10 coefficients per element and per mode. These coefficients are independent of the speed of the moving loads, and therefore, need not be recalculated if an analysis for different values of speed is to be carried out.

(2) Apart from numerical roundoff errors, the only approximation introduced in the procedure comes from the spatial discretization of the beam, which is inherent to any Finite Element model. The beam is discretized using two-noded Bernoulli–Euler elements of variable cross-section. Two degrees of freedom per node are considered (the vertical displacement and the slope).

(3) A time step is required in order to evaluate the solution and obtain a representation of the response time-history. Nevertheless, the equations of motion are integrated analytically, and therefore the response computed at any given time instant is not affected by the size of the step.

(4) At any fixed time instant, each modal amplitude is computed as the sum of two contributions: first, the one corresponding to the loads inside the beam (a fixed number of floating point operations per load is required), and second, a damped-sinusoidal oscillation that accounts for all the loads that have already left the structure.

(5) The semi-analytic procedure presented herein can be applied for the analysis of simply supported as well as continuous multi-span beams. The method is applicable to continuous beams with any number of spans of different lengths. Simultaneously, it allows for variable cross-section properties, which are usual in real structures.

(6) Implemented in a FORTRAN computer code running on a standard desktop PC, the method has proved to be computationally efficient, which makes it particularly useful for the design of actual bridges, allowing structural engineers to evaluate and compare the performance of different alternatives quickly and efficiently.

Acknowledgements

The authors wish to express their gratitude to Professor Rafael Gallego (Head of the Department of Structural Mechanics, University of Granada) for his help and encouragement during the development of this investigation, and also to Professor Ranjan Banerjee (City University of London) for the encouragement received at the CST-2004 conference in Lisbon.

Appendix A. Expressions for the coefficients of the mass and stiffness elemental matrices

A.1. Mass matrix coefficients

The coefficients of the consistent mass matrix are the following:

$$m^e_{11} = l^e\left(\frac{2m^e_i}{7}+\frac{3m^e_j}{35}\right),$$

$$m^e_{12} = (l^e)^2\left(\frac{m^e_i}{28}+\frac{m^e_j}{60}\right),$$

$$m^e_{13} = \frac{9l^e}{140}\left(m^e_i+m^e_j\right),$$

$$m^e_{14} = -(l^e)^2\left(\frac{m^e_i}{60}+\frac{m^e_j}{70}\right),$$

$$m^e_{22} = (l^e)^3\left(\frac{m^e_i}{168}+\frac{m^e_j}{280}\right),$$

$$m^e_{23} = (l^e)^2\left(\frac{m^e_i}{70}+\frac{m^e_j}{60}\right),$$

$$m^e_{24} = -\frac{(l^e)^3}{280}\left(m^e_i+m^e_j\right),$$

$$m_{33}^e = l^e\left(\frac{3m_i^e}{35}+\frac{2m_j^e}{7}\right),$$
$$m_{34}^e = -(l^e)^2\left(\frac{m_i^e}{60}+\frac{m_j^e}{28}\right),$$
$$m_{44}^e = (l^e)^3\left(\frac{m_i^e}{280}+\frac{m_j^e}{168}\right). \tag{A.1}$$

A.2. Stiffness matrix coefficients

The coefficients of the stiffness matrix are the following:

$$k_{11} = \frac{E[A_i^e(7(d_i^e)^2+2(d_i^e)(d_j^e)+(d_j^e)^2)+A_j^e((d_i^e)^2+2(d_i^e)(d_j^e)+7(d_j^e)^2)]}{20(l^e)^3},$$
$$k_{12} = \frac{E[A_i^e(15(d_i^e)^2+4(d_i^e)(d_j^e)+(d_j^e)^2)+2A_j^e((d_i^e)^2+(d_i^e)(d_j^e)+3(d_j^e)^2)]}{60(l^e)^2},$$
$$k_{13} = -\frac{E[A_i^e(7(d_i^e)^2+2(d_i^e)(d_j^e)+(d_j^e)^2)+A_j^e((d_i^e)^2+2(d_i^e)(d_j^e)+7(d_j^e)^2)]}{20(l^e)^3},$$
$$k_{14} = \frac{E[2A_i^e(3(d_i^e)^2+(d_i^e)(d_j^e)+(d_j^e)^2)+A_j^e((d_i^e)^2+4(d_i^e)(d_j^e)+15(d_j^e)^2)]}{60(l^e)^2},$$
$$k_{22} = \frac{E[A_i^e(33(d_i^e)^2+10(d_i^e)(d_j^e)+2(d_j^e)^2)+A_j^e(5(d_i^e)^2+4(d_i^e)(d_j^e)+6(d_j^e)^2)]}{180l^e},$$
$$k_{23} = -\frac{E[A_i^e(15(d_i^e)^2+4(d_i^e)(d_j^e)+(d_j^e)^2)+2A_j^e((d_i^e)^2+(d_i^e)(d_j^e)+3(d_j^e)^2)]}{60(l^e)^2},$$
$$k_{24} = \frac{E[A_i^e(12(d_i^e)^2+2(d_i^e)(d_j^e)+(d_j^e)^2)+A_j^e((d_i^e)^2+2(d_i^e)d_2+12(d_j^e)^2)]}{180l^e},$$
$$k_{33} = \frac{E[A_i^e(7(d_i^e)^2+2(d_i^e)(d_j^e)+(d_j^e)^2)+A_j^e((d_i^e)^2+2(d_i^e)(d_j^e)+7(d_j^e)^2)]}{20(l^e)^3},$$
$$k_{34} = -\frac{E[2A_i^e(3(d_i^e)^2+(d_i^e)(d_j^e)+(d_j^e)^2)+A_j^e((d_i^e)^2+4(d_i^e)(d_j^e)+15(d_j^e)^2)]}{60(l^e)^2},$$
$$k_{44} = \frac{E[A_i^e(6(d_i^e)^2+4(d_i^e)(d_j^e)+5(d_j^e)^2)+A_j^e(2(d_i^e)^2+10(d_i^e)(d_j^e)+33(d_j^e)^2)]}{180l^e}. \tag{A.2}$$

References

[1] L. Frýba, Dynamic behaviour of bridges due to high-speed trains, in: R. Delgado, R. Calçada, A. Campos (Eds.), *Workshop Bridges for High-Speed Railways*, Faculty of Engineering, University of Porto, 2004, pp. 137–158.

[2] F. Mancel, Cedypia: analytical software for calculating dynamic effects on railway bridges, in: *Proceedings of the Fourth European Conference on Structural Dynamics (Eurodyn '99)*, Prague, Czech Republic, 1999, pp. 669–674.

[3] F. Bleich, *Theorie und Berechnung der Eisernen Brücken*, Springer, Berlin, 1924.

[4] L. Frýba, *Vibration of Solids and Structures Under Moving Loads*, third ed., Thomas Telford, 1999.

[5] L. Frýba, A rough assessment of railway bridges for high speed trains, *Engineering Structures* 23 (2001) 548–556 (doi:10.1016/S0141-0296(00)00057-2).

[6] J. Li, M. Su, The resonant vibration for a simply supported girder bridge under high-speed trains, *Journal of Sound and Vibration* 224 (1999) 897–915 (doi:10.1006/jsvi.1999.2226).

[7] Y.B. Yang, J.D. Yau, L.C. Hsu, Vibration of simple beams due to trains moving at high speeds, *Engineering Structures* 19 (11) (1997) 936–944 (doi:10.1016/S0141-0296(97)00001-1).

[8] J.A. Gbadeyan, S.T. Oni, Dynamic behaviour of beams and rectangular plates under moving loads, *Journal of Sound and Vibration* 182 (1995) 667–695 (doi:10.1006/jsvi.1995.0226).

[9] M. Olsson, On the fundamental moving load problem, *Journal of Sound and Vibration* 145 (1991) 299–307 (doi:10.1016/0022-460X(91)90593-9).
[10] T. Hayashikawa, N. Watanabe, Dynamic behavior of continuous beams with moving loads, *Journal of the Engineering Mechanics Division, ASCE* 107 (1981) 229–246.
[11] Y.H. Chen, C.Y. Li, Dynamic response of elevated high-speed railway, *Journal of Bridge Engineering* 5 (2000) 124–130.
[12] K. Henchi, M. Fafard, G. Dhatt, M. Talbot, Dynamic behaviour of multi-span beams under moving loads, *Journal of Sound and Vibration* 199 (1) (1997) 33–50 (doi:10.1006/jsvi.1996.0628).
[13] Y.A. Dugush, M. Eisenberger, Vibrations of non-uniform continuous beams under moving loads, *Journal of Sound and Vibration* 254 (5) (2002) 911–926 (doi:10.1006/jsvi.2001.4135).
[14] C.W. Cai, Y.K. Cheung, H.C. Chan, Dynamic response of infinite continuous beams subjected to a moving force, *Journal of Sound and Vibration* 123 (1988) 461–472.
[15] J.S. Wu, C.W. Dai, Dynamic responses of multispan nonuniform beam due to moving loads, *Journal of Structural Engineering* 113 (1987) 458–474.
[16] H.P. Lee, Dynamic response of a beam with intermediate point constraints subject to a moving load, *Journal of Sound and Vibration* 171 (1994) 361–368 (doi:10.1006/jsvi.1994.1126).
[17] D.Y. Zheng, Y.K. Cheung, F.T.K. Au, Y.S. Cheng, Vibrations of multi-span non-uniform beams under moving loads by using modified beam vibration functions, *Journal of Sound and Vibration* 212 (1998) 455–467 (doi:10.1006/jsvi.1997.1435).
[18] K.J. Bathe, *Finite Element Procedures*, Prentice-Hall, Englewood Cliffs, NJ, 1996.
[19] European Committee for Standardization (CEN), Eurocode 1: actions on structures—Part 2: traffic loads on bridges, Final Draft prEN 1991-2, 2002.
[20] European Committee for Standardization (CEN), EN 1990—Eurocode: basis of structural design—Annex A2: application for bridges, Final PT Draft EN 1990—prAnnex A2, 2002.